Naval Research Laboratory

Washington, DC 20375-5320

NRL/MR/5673--99-8418

The Use of Fiber Bragg Grating Strain Sensors in Laboratory and Field Load Tests: Comparison to Conventional Resistive Strain Gages

MICHAEL TODD
LEX MALSAWMA
C.C. CHANG
GREGG JOHNSON

Optical Techniques Branch
Optical Sciences Division

November 12, 1999

REPORT DOCUMENTATION PAGE

Form Approved
OMB No. 0704-0188

1. AGENCY USE ONLY (*Leave Blank*)	2. REPORT DATE	3. REPORT TYPE AND DATES COVERED
	November 12, 1999	

4. TITLE AND SUBTITLE

The Use of Fiber Bragg Grating Strain Sensors in Laboratory and Field Load Tests: Comparison to Conventional Resistive Strain Gages

5. FUNDING NUMBERS

6. AUTHOR(S)

Michael Todd, Lex Malsawma, C.C. Chang, and Gregg Johnson

7. PERFORMING ORGANIZATION NAME(S) AND ADDRESS(ES)

Naval Research Laboratory
Washington, DC 20375-5320

8. PERFORMING ORGANIZATION REPORT NUMBER

NRL/MR/5673--99-8418

9. SPONSORING/MONITORING AGENCY NAME(S) AND ADDRESS(ES)

Naval Surface Warfare Center
Arlington, VA 22217

10. SPONSORING/MONITORING AGENCY REPORT NUMBER

11. SUPPLEMENTARY NOTES

12a. DISTRIBUTION/AVAILABILITY STATEMENT

Approved for public release; distribution unlimited.

12b. DISTRIBUTION CODE

13. ABSTRACT (*Maximum 200 words*)

Two tests, one involving a bent beam in the laboratory and one involving tensile testing of a ship hull substructure at Naval Surface Warfare Center/Carderock, were performed where strain readings were compared between conventional resistive strain gages (RSGs) and optical fiber Bragg gratings (FBGs). The closely matched results indicate the utility of FBG strain monitoring systems in the structural health field.

14. SUBJECT TERMS

Load tests Strain sensors
Fiber optics
Bragg gratings

15. NUMBER OF PAGES

14

16. PRICE CODE

17. SECURITY CLASSIFICATION OF REPORT	18. SECURITY CLASSIFICATION OF THIS PAGE	19. SECURITY CLASSIFICATION OF ABSTRACT	20. LIMITATION OF ABSTRACT
UNCLASSIFIED	UNCLASSIFIED	UNCLASSIFIED	SAR

NSN 7540-01-280-5500

Standard Form 298 (Rev. 2-89)
Prescribed by ANSI Std 239-18
298-102

Contents

The Use of Fiber Bragg Grating Strain Sensors in Laboratory and Field Load Tests: Comparison to Conventional Resistive Strain Gages

1. Fiber Bragg Grating Strain Sensors and Systems

Significant attention has been focused in recent years on the importance of structural health monitoring. Real-time assessments of deteriorating structures can provide valuable information regarding service-life evolution and may even yield clues towards preventative maintenance procedures. Many structural management programs involve visual inspection-based approaches, where assessment of structural health is made relatively infrequently due to the time and cost incurrence of accurate expert inspection of large structures. In addition to the paucity of data obtained in this fashion, useful structural condition assessments are often difficult to obtain if the degradation mechanism does not visually manifest itself. As a result, significant research in the field has turned towards developing emerging technologies as potentially powerful component of infrastructure management programs.

One important step in any structural management program is specifying the data and data collection system necessary. Technological approaches along these lines have focused previously, for the most part, on distributed strain and/or acceleration measurements, using on the order of 10-20 conventional gages; such relatively sparse populations can be insufficient in properly interrogating the dynamics of many large structures. More recently, the development and maturation of fiber optic sensor technology, particularly fiber Bragg grating (FBG) strain sensors, has provided a viable alternative sensing method, offering advantages such as electromagnetic immunity, light weight, small size, low transmission loss, self-telemetry, and corrosion resistance. Such FBG devices, when combined with appropriate demultiplexing strategies, have already been deployed successfully in a number of structural sensing applications [1, 2, 3, 4, 5, 6, 7].

FBG strain sensors are especially useful in these structural-grade sensing applications due to their inherent wavelength-encoded operation, where strain information from the sensing element is contained in the reflected light wavelength spectrum. Gratings are fabricated by focusing coherent ultraviolet light on a small section (typically 1 cm long) of optical fiber at a prescribed incident angle (Figure 1(a)). This process induces a periodic modulation in the fiber core local index of refraction such that the grating acts as a narrow-band optical wavelength filter, with light being reflected backwards at a wavelength dependent on

Manuscript approved October 27, 1999.

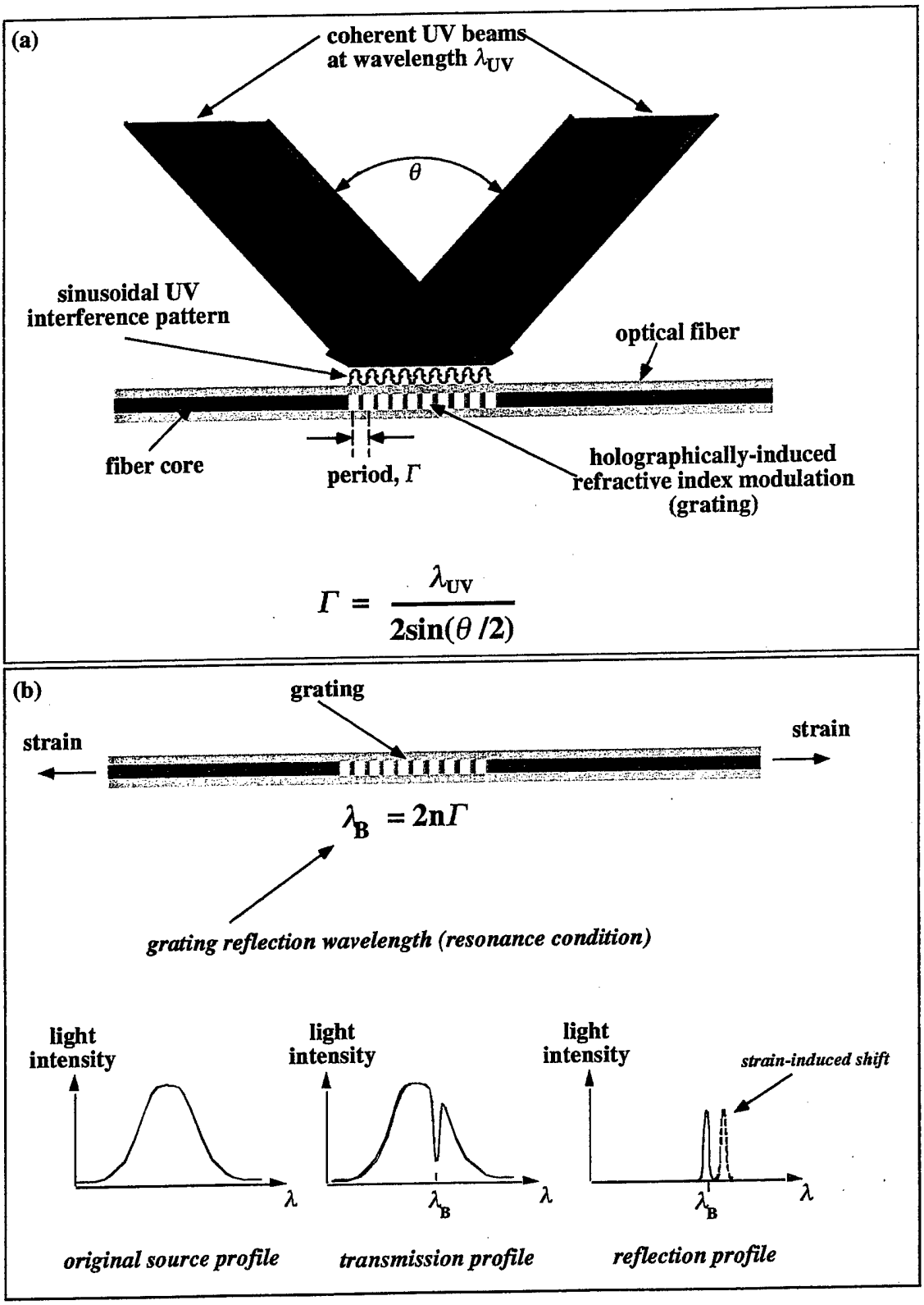

Figure 1. (a) Fabrication of fiber Bragg gratings with coherent ultraviolet illumination; (b) reflected wavelength shifts are attributable to strain at the grating location.

the modulation periodicity which is determined, in part, by the original incident angle of applied ultraviolet light (Figure 1(b)). This tunable wavelength encoding allows for easy multiplexing of many FBGs on a single optical fiber strand; each FBG can be manufactured to reflect light at a unique initial wavelength, corresponding to a unique location on the structure, and any reflected wavelength shift can be attributed to strain at that location (Figure 2(a)) in accordance with the strain/optic relationship

$$\Delta\lambda_B = (1 - p_e)\lambda_B \Delta\epsilon, \tag{1}$$

where $\Delta\lambda_B$ is the wavelength shift, $p_e \approx 0.22$ is the effective photoelastic constant, and $\Delta\epsilon$ is the change in strain.

Various research efforts have developed a number of real-time wavelength shift detection techniques capable of demultiplexing large FBG arrays [8], and the system used in this report utilized a scanning Fabry-Perot (FP) filter [9]; the total system schematic is shown in Figure 2(b) for a 64-channel architecture[1], including a performance characteristics summary and a photograph of the system package. It utilizes four diodes (ELEDs) as sources of light, six couplers, two FP filters, two photodetectors, electronic parts, and a laptop computer. The light emitted by the diodes and then reflected back from the sensor array is put through the filters, which pass only a very narrow band wavelength that is dependent upon the spacing between mirrors in the device. This spacing, and thus the passband, is controlled by applying a rapidly stepped voltage to a PZT driving the mirrors. The passed light signal is sent through a photodetector and differentiated; the zero-crossings of the differentiated signal correspond to the peak wavelengths of the reflected light, and correlation between the ramp voltage level and shifts in the zero-crossings results in obtaining the strain for each sensor, since wavelength shifts are proportional to strain in the grating (equation (1)). The FP filters used in this example had a free spectral range of about 45 nm, thus allowing a maximum of 16 individual sensors, spaced by approximately 2.7 nm, to be interrogated per filter scan. This spacing is sufficient to allow strains of about 1300 $\mu\epsilon$ for each grating to be monitored, if desired. The resolution of the voltage ramp and the free spectral range of the filters primarily determine the optimal strain resolution (minimum detectable strain) as well; for the current system, strain resolution on the order of 1-2 $\mu\epsilon$ is possible,

[1]Despite the high channel count capability, only one to three channels were used for the tests described in this report.

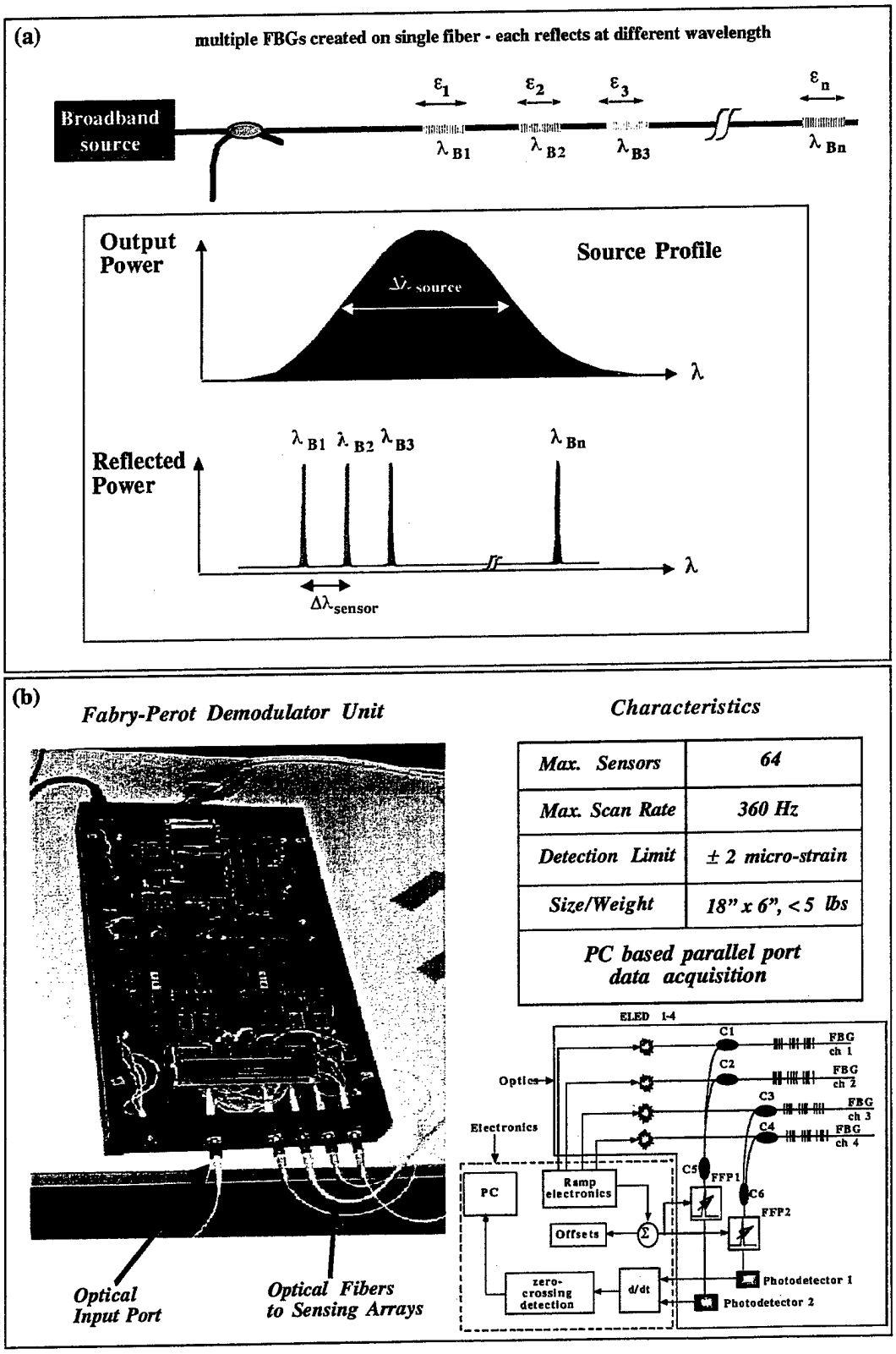

Figure 2. (a) Wavelength division multiplexing (WDM) strategy; (b) NRL Fabry-Perot WDM system, including schematic and performance characteristics.

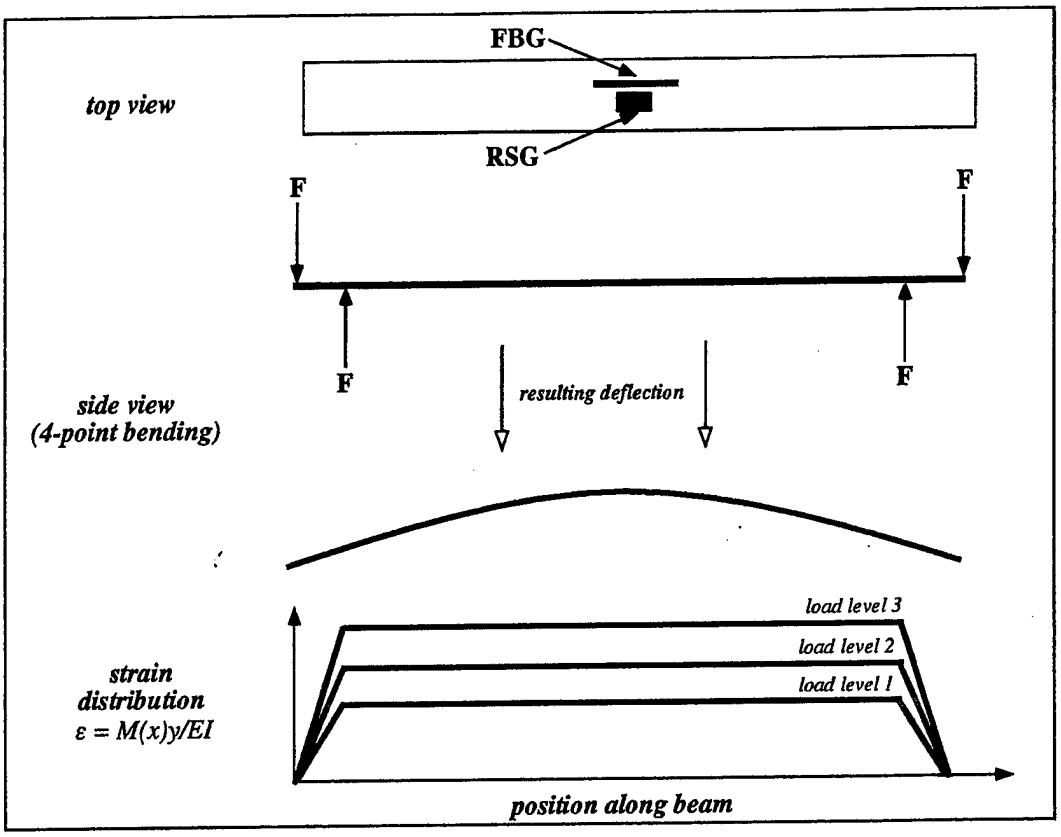

Figure 3. An RSG and an FBG were affixed to the surface of a beam loaded in a four-point bending apparatus.

although electronic noise can degrade the resolution to approximately 10-15 $\mu\epsilon$ in some rare cases. For the FP filters used, the ramp voltage can be applied at 360 Hz (a 180 Hz data acquisition rate under the Nyquist criterion), but the array in this work was set to acquire data at approximately 8 Hz by averaging to obtain better resolution. The relatively static nature of the tests performed in this report dictated that an 8 Hz sampling rate is more than adequate. Finally, temperature compensation, if needed, can be performed by utilizing gratings which are not mechanically coupled to the structure such that appropriate differencing would eliminate thermally-induced strain.

2. Beam Four-Point Bending Test

As an initial laboratory test for comparing FBG strain response to conventional RSG response, a simple beam was loaded on a four-point bending apparatus (Figure 3). This

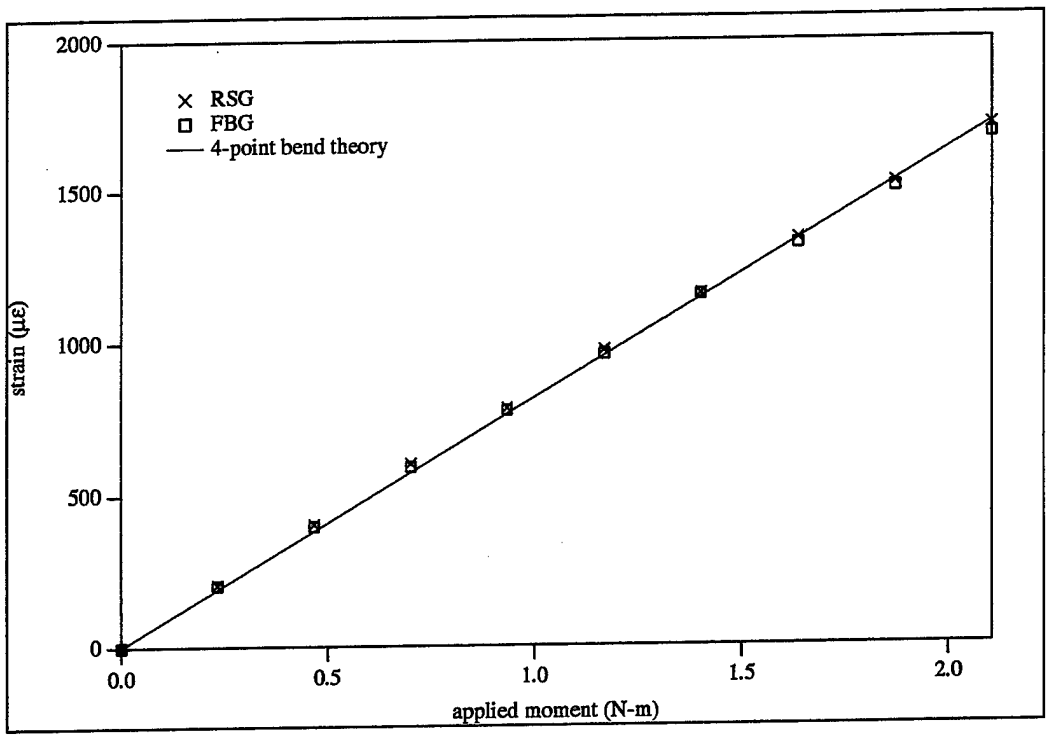

Figure 4. Strain response comparison between an FBG and an RSG strain gage, along with expected four-point bending theory.

loading arrangement results in a uniform moment distribution along the beam between the middle two loading locations, as shown at the bottom of the figure; as the magnitude of load P increases, the moment distribution evolves as shown. With elementary beam theory, axial strain ϵ is proportional to the moment:

$$\epsilon = \frac{M(x)y}{EI}, \tag{2}$$

where $M(x)$ is the moment distribution, y is the normal distance away from the neutral axis of the beam, E is Young's modulus, and I is the area moment of inertia. The reason for choosing a loading scenario which provides a region of constant moment is that the resulting strain, in accordance with equation (2), is also constant such that sensor gage lengths are irrelevant. Conversely, if the moment is varying, the strain gages sense an *average* strain over the active gage length, and because the FBG and RSG sensors are different sizes, optimal comparison is not achievable.

The beam chosen was aluminum (E=70 GPa) with dimensions 36.6 cm long, 3.8 cm wide, and 0.156 cm thick. As the load (and subsequent moment) was increased from zero, the results are shown in Figure 4, along with the theoretical four-point bending result from

elementary beam theory. The results agree very well across the loading band. The very slight variations between the RSG and FBG (typically a few $\mu\epsilon$) could result from a couple sources:

- The fiber core recoating process required during grating fabrication sometimes leaves asymmetries in the fiber coating, resulting in minor strain transfer variations between the core and the beam;
- Either the RSG or the FBG or both may not be bonded to the beam in an ideal way;
- The distance y from the neutral axis of the beam to each sensor's active zone may differ slightly.

Despite these possible error sources, the difference between the RSG and the FBG throughout the test remained below 2%.

3. Hull Substructure Test

In this test, a steel hull substructure was planned to be compressed to the point of buckling and then slowly tension-cycled with increasing load amplitude until failure. The structure itself was approximately 7.3 m long and 2.0 m wide with four rows of stiffening ribs running along the long dimension, equally spaced, and two rows running along the short dimension, equally spaced. A total of fifty-six conventional RSG gages were bonded to the structure at various "critical" locations by NSWC personnel, and three FBGs were placed on the structure as near as possible to three corresponding RSGs; the locations of the FBG sensors are shown in Figure 5(a). One gage was placed at the center of the structure, one was placed directly over a stiffener to the left, and the third was placed along the long dimensional centerline further towards on edge. Furthermore, a fourth grating was left unbonded to the structure to serve as a temperature reference gage. The gratings were attached to the structure first by sanding and polishing the structure surface to a fine finish, cleaning it with alcohol, and using M-bond 200 adhesive. Although not done on this test, many previous applications, as in [3], involved a final step of overbonding each grating again with a five-minute epoxy, primarily for protection purposes.

Due to loading equipment failure, the intended compression/cyclic tension tests could not be performed, and only two tension cycles to 6.67 MN were completed. The results

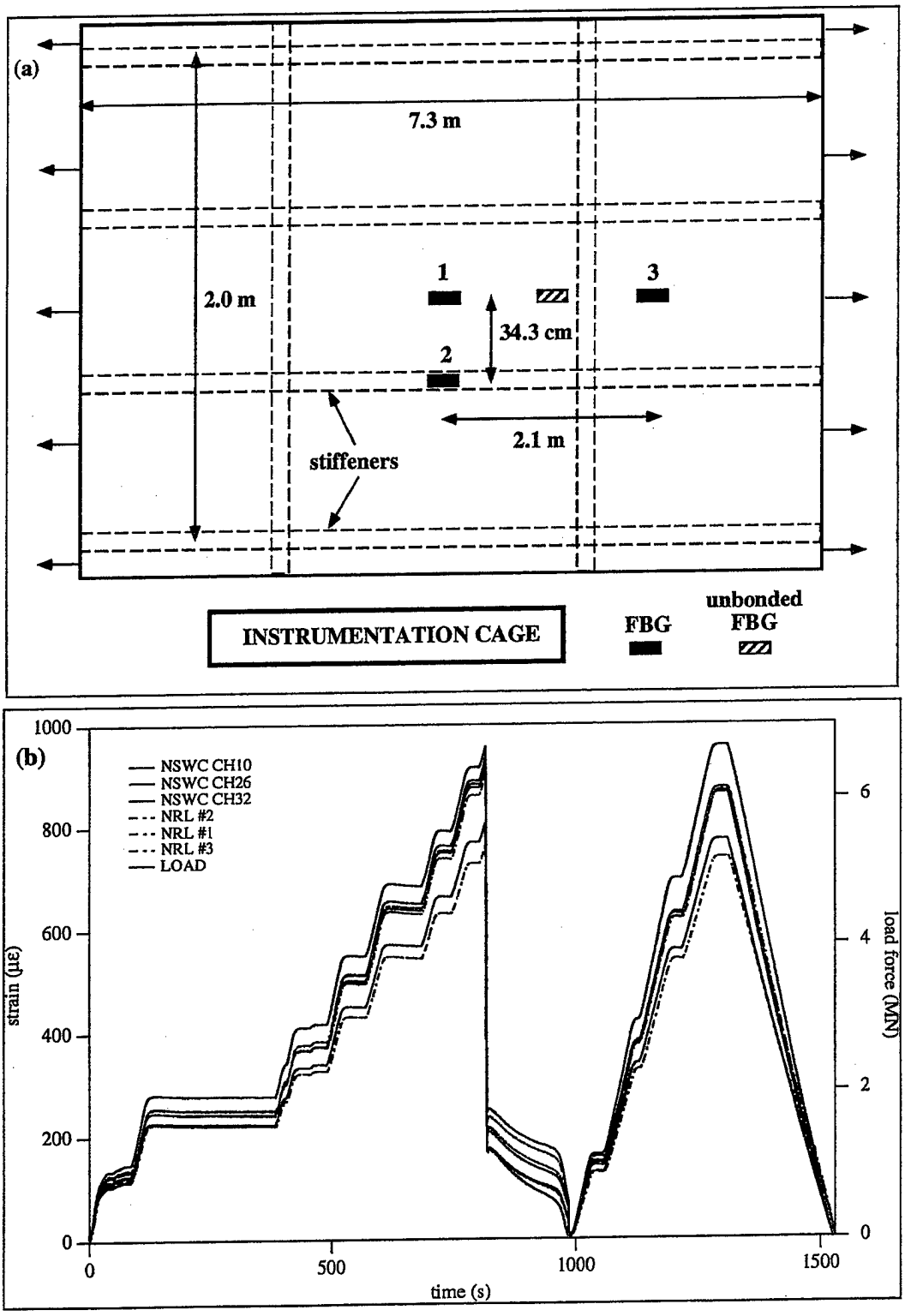

Figure 5. (a) A schematic of the hull substructure put through a tensile load test along with the placement of FBG sensors; (b) A comparison of FBG and RSG strain responses during the hull substructure tension cycles; applied absolute pre-strain to the gratings was removed for display purposes.

are shown in Figure 5(b). Both loadings were achieved in steps over approximately 750 seconds; in the first test, the load limit of the tensile machine was exceeded, and the force was released quickly rather than stepped down. The agreement between the RSG and FBG sensors at all three locations is quite good, and there is no hysteresis. The small deviations, observable primarily at high load magnitudes, are very likely due to FBG bonding issues. Because the initial test plan involved expected significant compression, approximately 2000-3000 $\mu\epsilon$ had to be imparted and held by hand during M-bond application and curing, and it is difficult to maintain tension and adhesive application uniformity. Such conditions may affect the expected strain transfer function. In addition, the FBG sensors were not exactly collocated with the RSG sensors, and any local strain concentrations or attenuations *e.g.*, local effects induced by the stiffeners, may not be detected by both sensor types. Despite these issues, the RSG sensors exactly mimic the qualitative trends of the FBG sensors with only slight quantitative discrepancy (always less than 5%) due to reasons just previously discussed.

4. Summary

One laboratory test with a bent beam and one field test with a steel ship hull substructure were performed whereby FBG strain sensors readings were compared to conventional RSG sensor readings. The FBG sensors closely matched the output of the RSG sensors, with minor errors typically attributable to FBG bonding issues. In addition, FBG sensors provide a number of unique advantages over conventional gages, *e.g.*, electromagnetic immunity, embeddability, self-telemetry, negligible invasiveness, and corrosion resistance, and are poised to make significant impact as the primary data collection component of structural monitoring systems.

5. Acknowledgments

The authors gratefully wish to acknowledge David Kihl and Bill Hay of NSWC for allowing NRL to take this opportunity to demonstrate the utility of FBG sensors.

References

[1] R. Maaskant, T. Alavie, R. M. Measures, G. Tadros, S. H. Rizkalla, and A. Guha-Thakurta. Fiber-optic Bragg Grating Sensors for Bridge Monitoring. *Cement and Concrete Composites*, 19:21–23, 1996.

[2] S. T. Vohra, C. C. Chang, B. A. Danver, B. Althouse, M. A. Davis, and R. Idriss. Preliminary Results on the Monitoring of an In-Service Bridge Using a 32-channel Fiber Bragg Grating Sensor System. In *Fiber Optic Sensors for Construction Materials and Bridges*. Technomic, 1998.

[3] M. D. Todd, C. C. Chang, G. A. Johnson, S. T. Vohra, J. W. Pate, and R. L. Idriss. Bridge Monitoring Using a 64-Channel Fiber Bragg Grating System. In *Proc. 17th Int. Modal Analysis Conf.*, pages 1719–1725, Orlando, FL, 1999.

[4] S. T. Vohra, M. D. Todd, G. A. Johnson, C. C. Chang, and B. A. Danver. Fiber Bragg Grating Sensor System for Civil Structure Monitoring: Applications and Field Tests. In *Proc. 13th Int. Conf. Optical Fiber Sensors*, pages 32–37, Kyongju, Korea, 1999.

[5] S. T. Vohra, G. A. Johnson, B. Danver, M. D. Todd, M. LeBlanc, and B. Althouse. Strain Monitoring During Construction of a Steel Box-Girder Bridge with Arrays of Fiber Bragg Grating Sensors. NRL report in preparation.

[6] M. D. Todd, G. A. Johnson, S. T. Vohra, C. C. Chang, B. Danver, and L. Malsawma. Civil Infrastructure Monitoring with Fiber Bragg Grating Sensor Arrays. In *Proc. 2nd Int. Workshop on Structural Health Monitoring*, Palo Alto, CA, (to appear September, 1999).

[7] G. A. Johnson, K. Pran, G. Wang, G. B. Havsgård, and S. T. Vohra. Structural Monitoring of a Composite Hull Air Cushion Catamaran with a Multi-Channel Fiber Bragg Grating Sensor System. In *Proc. 2nd Int. Workshop on Structural Health Monitoring*, Palo Alto, CA, 1999 (to appear September, 1999).

[8] A. D. Kersey, M. A. Davis, H. J. Patrick, M. LeBlanc, K. P. Koo, C. G. Askins, M. A. Putnam, and E. J. Friebele. Fiber Grating Sensors. *J. Lightwave Technol.*, 15:1442–1463, 1997.

[9] A. D. Kersey, T. A. Berkoff, and W. W. Morey. Multiplexed Fiber Bragg Grating Strain-Sensor System with a Fiber Fabry-Perot Wavelength Filter. *Optics Letters*, 18:1370–1372, 1993.